Ab initio simulation of the two-dimensional vibrational spectrum of dicarbonylacetylacetonato rhodium(I)

Andrew M. Moran, Jens Dreyer,[a] and Shaul Mukamel[b]
Department of Chemistry, University of Rochester, Rochester, New York 14627-0216

(Received 12 August 2002; accepted 21 October 2002)

The complete anharmonic cubic and quartic force field of the two carbonyl stretching vibrations of a rhodium di-carbonyl complex is calculated at the density functional level and used to simulate the third-order vibrational response function. The infrared photon echo spectrum calculated using the diagonalized resulting exciton Hamiltonian is in qualitative agreement with measured values. Quartic terms in the potential are critical for reproducing the experimental transition energies and transition dipoles. © *2003 American Institute of Physics.* [DOI: 10.1063/1.1528605]

I. INTRODUCTION

The structure of molecules is the primary basis for understanding and predicting their physical, chemical, biological, and material properties. An arsenal of multipulse nuclear magnetic resonance (NMR) techniques have been established and used for structure determination.[1–3] In recent years, IR analogs to NMR pulse sequences have been developed and applied to several model systems such as small peptides, acetone, and acetonitrile.[4,5] As in NMR, the power of nonlinear vibrational techniques is derived from the resolution of features not attainable in congested linear spectra, achieved by spreading the spectra out in multiple dimensions.[4–10] In addition, nonlinear IR spectroscopy has the potential to provide information regarding the time evolution of molecular structures on the subpicosecond time scale, in contrast to the millisecond regime directly accessible in NMR experiments.[4,6]

The NMR spin Hamiltonian is well-established, and its parameters are sufficiently transferable between different systems that spectral analysis is facilitated.[5,6,11] Conversely, anharmonic terms in the vibrational Hamiltonian need to be identified on a case by case basis in order to derive structural information from the measured spectra; the transferability of these parameters remains an open problem. Because nonlinear IR spectroscopies are sensitive to these anharmonic terms, their extraction should allow the interpretation of spectral features in terms of molecular geometry.[10–22]

To date, the most promising structurally sensitive nonlinear IR techniques have involved manipulation of incident pulse polarizations. Specifically, polarization selective measurements have been used to calculate angles between transition dipoles, which are interpretable in the molecular frame.[13,23–25] In addition, energies and amplitudes of vibrational peaks have been related to properties of the ground state potential energy surface.[9] In Ref. 25, a fitting procedure was used to invert the nonlinear spectrum of dicarbonylacetylacetonato rhodium(I) (RDC) (Fig. 1) into the parameters describing the two local carbonyl oscillators, as opposed to delocalized normal coordinates.

Information has thus far been obtained from experimental nonlinear spectra largely by using empirical fitting algorithms which require the selection of an optimal parameter set, using a model comprised of only the most important terms. Assumptions regarding the truncation of the expansion of the potential energy and transition dipole are unavoidable in the absence of an established microscopic understanding of the relative importance of these terms and their spectroscopic signatures.[25] Thus, we aim to simulate and predict nonlinear vibrational spectra without having to rely on input parameters from experimental sources. In this article we present a procedure for simulating nonlinear vibrational spectra based on *ab initio* electronic structure calculations. By developing a methodology that is generally applicable to small as well as to larger systems like biomolecules, our method will allow us to adapt the level of theory to the specific system under investigation in terms of balancing accuracy and computational cost. Exciton models[26–29] are especially promising in this regard provided that an appropriate scheme can be devised to transfer local *ab initio* parameters to larger systems which are intractable by high-level quantum mechanical methods.[28]

Being a well-studied and rigid molecule, RDC is an ideal candidate for the first application of this machinery. The symmetric and antisymmetric stretching vibrations of its two strongly coupled C≡O local oscillators are sufficiently separated from other absorption bands that their nonlinear response can be measured without contributions from other modes. The parameters needed to calculate the photon echo spectrum of RDC are generated at the density functional theory (DFT) level with the B3LYP[30–33] density functional and the LanL2DZ[34–36] basis set. Terms in the expansion of the potential energy to cubic order obtained via a fit of an experimental photon echo spectrum of RDC[25] provide a suitable reference for our calculations. In addition, we calculate quartic terms in the Hamiltonian and evaluate their effect on

[a]Present address: Max-Born-Institut für Nichtlineare Optik und Kurzzeitspektroskopie, D-12489 Berlin, Germany.
[b]Author to whom all correspondence should be addressed; Electronic mail: mukamel@chem.rochester.edu

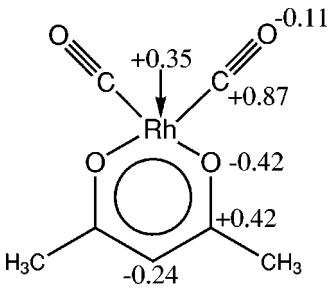

FIG. 1. RDC molecule: $(O{\equiv}C)_2Rh(O_2C_5H_7)$ and atomic Mulliken charges calculated at the B3LYP/LanLDZ level.

the nonlinear spectra by calculating transition energies and dipoles.

In order to connect spectra with local structural properties, the Hamiltonian should be set up in a basis of localized coordinates. Normal modes are easily obtained from standard quantum-chemical codes and represent a common choice for the calculation of harmonic as well as anharmonic vibrational spectra. Even though they are inherently delocalized,[37] they may be localized by procedures analogous to localization methods developed for molecular orbitals[38] or the construction of Wannier excitons in solid-state physics.[39] However, we have chosen to calculate the Hamiltonian directly in a basis of localized internal coordinates (see Sec. II). As a full calculation of all $3N-6$ coordinates is numerically expensive, a subset of internal coordinates of interest is selected. This selection can be based on the specific structural or spectral properties to be investigated. Remaining coordinates as well as environmental (bath) degrees of freedom determine the line shapes of nonlinear spectra. In the present study, we focus on simulating and analyzing the primary spectral features and line broadening is taken into account by simply adding a homogeneous linewidth. Bath effects may be incorporated microscopically in future studies.[40]

The accuracy of *ab initio* quantum chemical calculations of nonlinear spectra is yet to be tested. The parameters necessary to simulate off-resonant optical,[41] IR,[42] and mixed Raman/IR two-dimensional spectra[43] of $CHCl_3$ were calculated using the Hartree–Fock method. With respect to normal coordinates, the cubic potential energy expansion coefficients and derivatives of both the dipole and polarizability to the second-order term in the Taylor series were calculated and inserted into the relevant response functions. Qualitative agreement was found with experimental measurements, and the various experiments were shown to be complementary with regard to information content. It was predicted that in both field regimes, optical and IR, the nonlinear response is dominated by mechanical rather than electrical anharmonic contributions. In other words, the cubic term in the potential energy expansion is of much greater importance for the nonlinear response than the quadratic term in the dipole expansion.[4,29]

Our calculation begins with a geometry optimization. The Hamiltonian is constructed as a Taylor series truncated at fourth order and expansion coefficients corresponding to gradients, quadratic, cubic, and quartic force constants are calculated. Second-order force constants are taken directly from Hessian calculations, whereas third- and fourth-order derivatives are determined numerically by finite differences. Local transition dipole moments are evaluated to first order. Diagonalization of the effective vibrational exciton Hamiltonian starting with a harmonic basis yields the energy levels and transition dipoles that are used to compute the vibrational spectra.

In Sec. II, the procedure used to construct the Hamiltonian of RDC, which explicitly includes the two carbonyl $(C{\equiv}O)$ bonds, is described. In Sec. III, the Hamiltonian is recast using normally ordered creation and annihilation operators. Section IV presents the calculated parameters and the corresponding two-dimensional photon echo spectrum. The calculated and experimental molecular and spectroscopic parameters are generally in good agreement, demonstrating that nonlinear vibrational spectra can be adequately simulated using *ab initio* methods.

II. *AB INITIO* COMPUTATION OF ANHARMONIC POTENTIAL ENERGY SURFACES

The potential energy V in the anharmonic vibrational Hamiltonian has been expanded to quartic order with respect to a selected subset of internal coordinates R_k as

$$H=V_0+\sum_m^{3N-6} f_m R_m+\sum_m^{3N-6}\frac{P_m^2}{2m_m}+\sum_{m,n}^{3N-6} f_{mn}R_mR_n+\sum_{m,n,p}^{3N-6} f_{mnp}R_mR_nR_p+\sum_{m,n,p,q}^{3N-6} f_{mnpq}R_mR_nR_pR_q, \tag{1}$$

where the nth order partial derivatives of the potential energy are given by

$$f^{(n)}_{k1k2\cdots kn}=\frac{1}{n!}\left(\frac{\partial^n V}{\partial R_{k1}\partial R_{k2}\cdots\partial R_{kn}}\right)_0. \tag{2}$$

The nuclear dipole required to calculate IR spectra is truncated at the linear order,

$$\vec{\mu}=\vec{\mu}_0+\sum_m^{3N-6}\left(\frac{\partial\vec{\mu}}{\partial R_m}\right)_0 R_m. \tag{3}$$

Anharmonic potential energy surfaces of large polyatomic molecules are usually determined by calculating anharmonic force constants defined as elements of a Taylor series [Eq. (1)] expansion around a reference geometry.[37] The expansions may be performed with respect to either Cartesian, internal, or normal coordinates. When the force constants are related to spectroscopic observables, normal modes are the most common choice. However, because normal modes are delocalized, it is difficult to relate them to microscopic (local) properties of the molecule. In contrast to Cartesian and internal coordinates, the mass-weighted normal modes only provide isotope-dependent force fields, limiting their generality. Thus, force constants must be recalculated for every isotopic derivative. Furthermore, delocalized force constants are not easily transferred from one molecule to another. Cartesian coordinates are well-defined and easy to

use, but molecular motion may be better visualized using internal coordinates. Internal coordinates such as bond lengths, bond angles, and dihedral angles are inherently localized, as they are confined to two, three, and four atoms, respectively. The resulting force constants are usually diagonally dominant and facilitate transfer and comparison between related molecules.[37] Isotope effects can be readily studied as effective masses for internal coordinates enter the vibrational Hamiltonian directly (*vide infra*).

Internal coordinates need to be provided as input for the quantum chemical calculations and should be carefully chosen for each molecule under investigation. It is advantageous to select the bond lengths and angles that best approximate the vibrational modes of interest, so that calculations can be interpreted in terms of physically meaningful local vibrations. If a molecule possesses some symmetry, the coordinates can be selected accordingly to simplify the interpretation. The reference geometry can be obtained either from (i) the optimum geometry at the level of theory used in the force field calculation, (ii) an optimum geometry at a higher level of theory, (iii) an empirically corrected theoretical, or (iv) an experimental x-ray or NMR geometry. Among these options the first appears to be most consistent and is adopted in our study.

The calculation of harmonic vibrational frequencies by Hartree–Fock-based methods, DFT,[44] and by molecular mechanics has recently been reviewed.[45] It has been shown that Hartree–Fock methods with at least split valence basis sets predict qualitatively correct force constants;[46,47] they contain systematic errors because of the neglect of electron correlation, which usually leads to an overestimation of vibrational frequencies by about 10%. Electron correlation can be taken into account by post-Hartree–Fock methods such as Møller–Plesset perturbation theory or configuration interaction. However, these procedures are computationally expensive and thus restricted to relatively small molecules. DFT includes electron correlation,[48] but is computationally much less demanding than post-Hartree–Fock methods and has thus developed into a general method to study physical properties of medium-sized molecules. BLYP and B3LYP functionals with polarized split valence basis sets have given the best agreement between calculated and experimental vibrational frequencies.[44,49–52] Compared to Hartree–Fock the deviation from experiment appears to be much more uniform. In fact, empirical frequency scaling factors of 0.99 and 0.96 have been reported for BLYP and B3LYP methods, respectively, whereas the corresponding Hartree–Fock scaling factor is 0.90.[46,47,53,54] Depending on the molecular class of interest, DFT methods gave average errors of 13,[49] 26,[50] 19,[50] and 34–45 cm^{-1}.[51] Average frequency errors are about 20–40 cm^{-1} larger for Hartree–Fock as well as for Møller–Plesset approaches.[51] Semiempirical methods exhibit considerably larger deviations with reported errors of 126 and 159 cm^{-1} for AM1 and PM3, respectively.[51] Quadratic configuration interaction calculations in which single and double substitutions are included are similar in quality to DFT, but they are not competitive with respect to computational cost.

Recently, the very good performance of DFT methods was demonstrated for the vibrations of compounds containing up to fourth-row elements or isotopes.[55] Large deviations were found only for molecules in which dispersion forces play a significant role, e.g., in molecules containing several halogen atoms. Complemented by a linear scaling method that corrects for anharmonic effects, high-quality DFT methods like B3LYP together with large basis sets like 6-311 $+G(d,p)$ appear to most accurately predict vibrational spectra.[55,56] However, the accuracy of DFT, as well as perturbative and certain truncated configuration interaction methods, with respect to the calculation of anharmonic force constants is questionable.[37] It has been found that Hartree–Fock methods are capable of predicting higher-order derivatives of the potential energy to within a few percent in the strongly bonding region of the potential energy surface.[37]

For large molecules like proteins or nucleic acids *ab initio* methods are still too expensive and one has to rely on mechanical force fields. If the parametrization is properly chosen, reasonable results can be expected from force field normal mode calculations.[45]

The accuracy of calculated vibrational intensities has not been systematically tested, as has already been done for frequencies.[57–60] Compared to frequencies, vibrational intensities are much more sensitive to the choice of the basis set. Medium or large basis sets, at least polarized split valence basis set, are needed to produce satisfactory results.[57] Inclusion of electron correlation improves quantitative predictions. In contrast to frequency predictions, there is no definite tendency in over- or underestimation of intensities.

We have used the standard quantum chemical packages GAMESS(US)[61] and GAUSSIAN 98[62] to calculate harmonic second-order force constants. Both programs construct the Hessian matrix in the basis of internal coordinates specified in the input. Preferably, quantum chemical methods with analytical first- and second-order derivatives[63] capabilities should be used to minimize numerical errors at this stage of the calculation.

We determined the cubic and quartic anharmonic force constants numerically, by calculating first- and second-order derivatives of analytical quadratic force constants. We used three- and five-point central difference formulas, as forward or backward formulas are known to be an order of magnitude less accurate.[37] In our experience, the change of the force constants in going from three-point to five-point formulas is rather small, but the computational effort is increased by a factor of 2. We thus restrict ourselves to three-point formulas. We found literature recommendations for displacement steps to be appropriate, namely 0.01 Å for bond lengths and 0.02 rad for angle displacements.[37] As we calculated only nonredundant force constants one should be aware that in the calculation of cubic (f_{mnp}) and quartic (f_{mnpq}) force constants the different treatment of the derivatives m and n (analytically or, e.g., in the case of semiempirical calculations, m analytically and n numerically) versus p and q (numerically) may lead to artificial asymmetries for cubic and quartic force constants that are actually identical by molecular symmetry. These are usually rather small, but we found that they may become appreciable for certain quartic force constants.

Numerical internal first-order dipole derivatives were

calculated concomitantly. It should be noted that rotation or distortion (displacements) of chemical bonds upon vibrations may cause the inertial axes to rotate with respect to the rest of the molecular structure. This can result in the permanent dipole moment giving a contribution to the transition moment. This artifact may affect the intensity of vibrational absorption bands, as was first pointed out by Crawford in 1952.[64] A procedure to overcome these complications and to perform such calculations accurately has recently been given by Ford and Steele.[65] They noticed, however, that in larger molecules these contributions only have a minor effect. Thus, in the present work we neglected these corrections to the calculated dipole derivatives.

III. THE NORMALLY ORDERED VIBRATIONAL EXCITON HAMILTONIAN

Numerical computations and the systematic classification of spectra can be better carried out by transforming the Hamiltonian to the second quantized normally ordered form. This also helps establish the connection with exciton models. To that end we transform the internal coordinates R_k and momenta P_k by bosonic creation $(B_k^\dagger)$ and annihilation (B_k) operators operators according to

$$R_k = \sqrt{\frac{\hbar}{2m_k\omega_k}}\,(B_k^\dagger + B_k), \tag{4}$$

$$P_k = i\sqrt{\frac{m_k\hbar\omega_k}{2}}\,(B_k^\dagger - B_k), \tag{5}$$

where m_k and ω_k represent effective masses and intrinsic frequencies of the internal coordinate R_k and $\hbar$ is Planck's constant. These operators satisfy the Bose commutation relation

$$[B_k, B_l^\dagger] = \delta_{kl}. \tag{6}$$

The Hamiltonian may be written in many different forms by changing the order of various $B_k^\dagger$ and B_k factors. It is convenient to adopt *normal ordering* where all $B_k^\dagger$'s are moved to the left and B_k's to the right. Neglecting the constant term and recognizing that the derivatives are invariant to permutations of the dummy indices, the vibrational Hamiltonian [Eq. (1)] becomes

$$\begin{aligned} H = & \sum_m^{3N-6} U_m(B_m^\dagger + B_m) \\ & + \sum_{m,n}^{3N-6} [h_{mn}B_m^\dagger B_n + U_{mn}(B_m^\dagger B_n^\dagger + B_m B_n)] \\ & + \sum_{mnp}^{3N-6} U_{mnp}(B_m^\dagger B_n^\dagger B_p^\dagger + 3\,B_m^\dagger B_n^\dagger B_p + 3\,B_m^\dagger B_n B_p \\ & + B_m B_n B_p) + \sum_{mnpq}^{3N-6} U_{mnpq}(B_m^\dagger B_n^\dagger B_p^\dagger B_q^\dagger \\ & + 4\,B_m^\dagger B_n^\dagger B_p^\dagger B_q + 6\,B_m^\dagger B_n^\dagger B_p B_q + 4\,B_m^\dagger B_n B_p B_q \\ & + B_m B_n B_p B_q), \end{aligned} \tag{7}$$

where the parameters of Eq. (7) are defined by Eqs. (A2)–(A7). The dipole operator is similarly given as

$$\vec{\mu} = \sum_m^{3N-6} D_m^{(1)}(B_m^\dagger + B_m). \tag{8}$$

The electronic excitations of molecular aggregates and crystals made out of similar repeat units are described by the Frenkel exciton Hamiltonian which bears a resemblance to Eq. (7). The main differences are that in the electronic case the creation and annihilation operators satisfy the Pauli rather than the Bose commutation rules. In addition, the Heitler–London approximation (couplings among units are weak compared to frequencies) allows one to retain only a few nonlinear terms in the Frenkel case. The vibrational Hamiltonian is more complex since many types of anharmonicities may be relevant. Nevertheless, many concepts and techniques such as Green functions and quasiparticle representations developed for electronic excitons may be applied for computing vibrational excitons. Pioneering studies of the structure of vibrational excitons[28,29] in pure and mixed crystals were made by Kopelman and co-workers.[66–68] More recently, they have also been studied in peptides.[69–71] The only realistic and logical strategy for modeling large molecules such as peptides or DNA will be to use quantum chemistry computations on small segments to construct an effective exciton Hamiltonian which can then be diagonalized.

IV. APPLICATION TO RDC

The anharmonic potential energy surface along the two carbon–oxygen triple bonds was constructed using the B3LYP[30–33] density functional and LanL2DZ basis set.[34–36] This method was selected because of its agreement with experimental frequencies and similarity to a method previously used to study the vibrations of rhodium complexes.[72] The LanL2DZ basis incorporates an effective core potential for the rhodium atom rather than treating all electrons explicitly, and uses the Dunning/Huzinaga full double zeta basis for the remaining atoms.[34–36] We have calculated anharmonic force constants for a selected subset of $(n=2)$ internal coordinates only.

The vibrational eigenstates were obtained by diagonalizing the Hamiltonian expanded in a harmonic basis set. The basis state wave function i is factorized into a product of local harmonic oscillators according to

$$|m_{i1}m_{i2}n_{i3}\cdots m_{in}\rangle = |m_{i1}\rangle|m_{i2}\rangle|m_{i3}\rangle\cdots|m_{in}\rangle, \tag{9}$$

where m denotes the number of vibrational quanta in local oscillator in. Matrix elements of the Hamiltonian are evaluated by application of the following rules:

$$\langle m_i|B_i^\dagger|n_i\rangle = \sqrt{n+1}\langle m_i|n_i+1\rangle = \sqrt{n+1}\,\delta_{m_i,n_i+1}, \tag{10}$$

$$\langle m_i|B_i|n_i\rangle = \sqrt{n}\langle m_i|n_{n-1}\rangle = \sqrt{n}\,\delta_{m_i,n_i-1}, \tag{11}$$

where m and n represent the number of vibrational quanta in the local oscillator i.

We should include a minimum number of three energy levels for each local vibrational coordinate to produce the singly and doubly excited eigenstate manifolds. Thus, our

two-coordinate model requires at least six states: a vibrational ground state, two singly excited states, two doubly excited states, and a combination band with one excitation in each coordinate. However, the energies of excited vibrational states do not converge with this minimum basis set, because coupling with higher excited states (more than two quanta) is needed to stabilize the singly and doubly excited levels. A similar effect is observed in the truncated configuration interaction electronic structure scheme, where the (dynamic) electron correlation energy is not sufficiently taken into account due to the truncation. Therefore, the manifold of basis states was expanded until convergence of the singly and doubly excited state energies and eigenvectors is achieved. In the present two-coordinate calculation, we truncated our manifold of basis states at thirteen vibrational quanta, i.e., the sum of the quanta among all local modes is thirteen. At each level of the manifold, all possible basis states are generated, resulting in one-hundred-five basis vectors.

Table I contains the parameters calculated at three approximation levels. The symmetrically equivalent C≡O bonds are denoted by the indices 1 and 2. The six lowest energy eigenstates consist of the vibrational ground state (g), the symmetric (s) and antisymmetric (a) singly excited vibrational states, as well as their two overtones (aa,ss), and a combination band (as). The parameters ω_k, Ω_j, Δ_{jj} are the intrinsic frequencies of the local C≡O oscillators, the frequency of the eigenmode, and the anharmonicity of the doubly excited states. The relations of the expansion coefficients [Eq. (A6)] to the parameters in the table are given in the footnotes of Table I. Transition dipoles are normalized to the transition dipole of the symmetric fundamental transition ($\mu_{g,s}$).

Results obtained by truncating the potential energy expansion at the third and fourth order are shown in columns two and four, respectively. In addition, the results of a calculation in which the off-diagonal third- and fourth-order expansion coefficients (coefficients involving more than one coordinate index) are neglected are given in column three. The *ab initio* parameters are compared with those of a fit to the experimental photon echo spectrum in which a two oscillator Hamiltonian was truncated at the cubic term.[25]

Intrinsic (ω_k) and eigenstate frequencies (Ω_j) of the two singly excited states are about 100 cm^{-1} below the experimental values. A harmonic normal mode analysis including all $3N-6$ coordinates at the same level of theory produces vibrational frequencies of 1972 and 2033 cm^{-1} for the respective modes, indicating that the lower frequencies are inherent in the level of calculation and not the result of using a subset of coordinates. Our calculated splitting between the two levels is 27.4 cm^{-1}, less than half the experimental value (69 cm^{-1}). Accordingly, the quadratic off-diagonal term V_{12} is less than half the size of the experimental V_{12} as well. Although most of the amplitude resides in the C≡O bonds, additional coordinates are needed to improve the bilinear coupling between the eigenmodes. Inclusion of the Rh–(CO) coordinates, which comprise less than 1% of the mode composition, produces a negligible change in the energy difference between the singly excited levels (27.5 cm^{-1}), indicating that the collective effect of many weakly coupled coordinates is significant.

In our fourth-order calculation, the anharmonicities (Δ_{jj}) deviate by less than 6 cm^{-1} from the measured values. Truncation at the cubic term results in anharmonicities that are much greater than those of experiment, by up to 41 cm^{-1}. The magnitudes (as well as the signs) of the cubic expansion coefficients (g_{iii}) show substantial deviations from the experimental fit. Quartic coefficients cannot be directly compared to experimental values because the Hamiltonian used to model the spectra was truncated at third order.[25] The calculated transition dipoles are in excellent

TABLE I. Calculated and empirically determined parameters.

Parameters[a]	Third order	Fourth-order diag	Fourth order	Empirical[b]
	Vibrational frequencies (cm^{-1})[c]			
ω_1 (local)	1974	1974	1974	2073.5
ω_2 (local)	1974	1974	1974	2073.5
Ω_a	1903.9	1922.8	1922.9	2015
Ω_s	1931.6	1950.5	1950.3	2084
Δ_{aa}	47	12.2	12.3	13
Δ_{ss}	16.7	7.9	8.2	12
Δ_{as}	61.6	20.1	20.3	26
	Expansion coefficients (cm^{-1})[d]			
V_{12}	13.6	13.6	13.6	35
g_{111}	−244.6	−244.6	−244.6	170
g_{112}	−0.5	0.0	−0.5	3
g_{122}	−0.5	0.0	−0.5	3
g_{222}	−244.6	−244.6	−244.6	170
g_{1111}	⋯	50.8	50.8	⋯
g_{1112}	⋯	0.0	0.0	⋯
g_{1122}	⋯	0.0	0.0	⋯
g_{1222}	⋯	0.0	0.1	⋯
g_{2222}	⋯	50.8	50.8	⋯
	Angle between transition dipoles (deg)			
Θ local	91.8	91.8	91.8	92
Θ eigenstates	92.2	92.3	94.2	90
	Transition dipoles (normalized to μ_s)[e]			
$\mu_{g,a}$	0.97	1.04	1.04	1.05
$\mu_{g,s}$	1.00	1.00	1.00	1.00
$\mu_{g,aa}$	0.06	0.05	0.05	⋯
$\mu_{g,ss}$	0.02	0.03	0.03	⋯
$\mu_{g,as}$	0.07	0.06	0.06	⋯
$\mu_{a,aa}$	1.35	1.45	1.45	1.48
$\mu_{s,ss}$	1.29	1.39	1.39	1.41
$\mu_{a,ss}$	0.61	0.27	0.27	0.13
$\mu_{s,aa}$	0.61	0.27	0.27	0.13
$\mu_{a,as}$	1.02	1.00	1.00	1.00
$\mu_{s,as}$	1.05	1.05	1.04	1.05

[a]The indices 1 and 2 denote local C≡O coordinates, whereas g, s, and a representing the ground state and the singly excited symmetric and antisymmetic eigenstates. The indices aa, ss, and as represent the two overtones and the combination band, respectively.

[b]Empirical fit of a cubic potential to the photon echo spectrum given in Ref. 3.

[c]The parameters ω_k, Ω_j, Δ_{jj} are the intrinsic frequency of the local oscillator, the frequency of the eigenmode, and the anharmonicity of the doubly excited state.

[d]The relation of the expansion coefficients [Eqs. (A2)–(A7)] to the parameters in the table are as follows: $V_{mn}=2\times U^{(2)}_{mn}$, $g_{mnp}=6\times U^{(3)}_{mnp}$, and $g_{mnpq}=24\times U^{(4)}_{mnpq}$.

[e]The transition dipoles are normalized to the transition dipole between the ground state and singly excited level of the symmetric stretching mode.

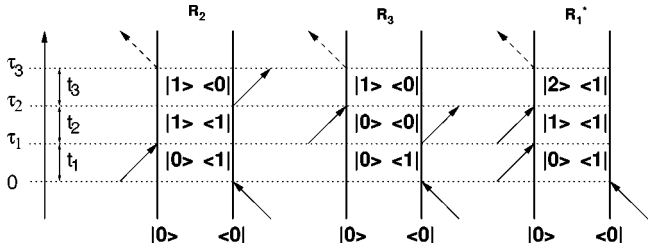

FIG. 2. Double-sided Feynman diagrams describing the third-order nonlinear response for the signal in the wave vector direction $\mathbf{k}_s=-\mathbf{k}_1+\mathbf{k}_2+\mathbf{k}_3$.

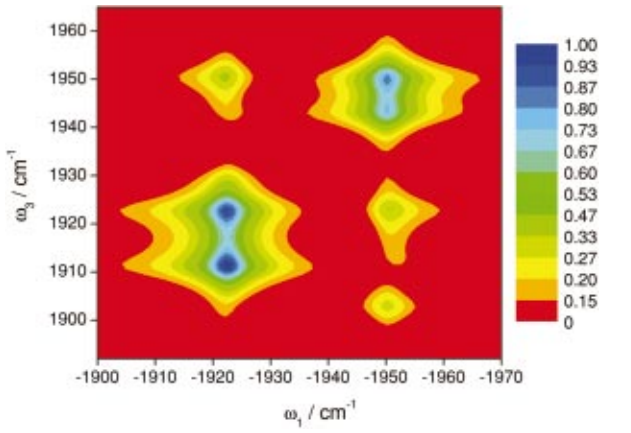

FIG. 3. (Color) Three pulse photon echo spectrum of RDC calculated using the parameters in column 4 of Table I, where all potential energy terms to fourth order are included. The axes labels ω_1 and ω_3 correspond to the respective time intervals. The plotted intensity represents the absolute value of $|S_{ZZZZ}(\omega_3,t_2=0,\omega_1)|$ [Eq. (13)]. The spectrum has been normalized to the maximum peak intensity.

agreement with the measurements, suggesting that nearly all of the oscillator strength of these transitions are associated with the two C≡O bonds. Transition dipoles calculated by truncating Eq. (8) at second order deviated by less than 1.2% from those found using only the linear term. It is therefore well justified to truncate the expansion of the dipole operator at the linear term for RDC.

Our results show a significant change in energies and anharmonicites due to the inclusion of fourth-order terms, resulting in a substantial reduction in the deviation from experimental values. The $g_{kkkk}(R_k^4)$ type terms are most important in this regard. This suggests that while a cubic truncation of the Hamiltonian includes enough parameters to fit experimental data, the effects of cubic and quartic expansion coefficients must be artificially combined in the cubic parameters. It is therefore not surprising that the magnitudes of the empirical third-order expansion coefficients differ so greatly from ours. While the difference in sign hardly affects the calculated energies, negative diagonal third derivatives are intuitive and more commonly encountered,[37] as they describe an increase in the intrinsic frequency of the bond as it decreases in length.

We have calculated the photon echo signal generated in the $\mathbf{k}_s=-\mathbf{k}_1+\mathbf{k}_2+\mathbf{k}_3$ direction using the sum over states expression.[29] The response function is given by the sum of three Liouville space pathways:[6]

$$R(t_3,t_2,t_1)=R_2(t_3,t_2,t_1)+R_3(t_3,t_2,t_1)-R_1^*(t_3,t_2,t_1). \tag{12}$$

The Liouville space paths are represented by the double-sided Feynman diagrams shown in Fig. 2. When the pulses are short relative to the system dynamics, the polarization $P^{(3)}$ is directly proportional to the response function. It is often most intuitive to view the signal in the frequency domain by Fourier transforming the polarization with respect to the relevant time variables. Orientational factors related to the angles between the transition dipoles and the polarizations of the four fields can be conveniently introduced by taking the orientational and vibrational part of $R(t_3,t_2,t_1)$ to be separable, and assuming the chromophore is fixed in the laboratory frame during the course of the experiment.[23] The nonlinear polarization is Fourier transformed with respect to t_1 and t_3,

$$S_{ijkl}(\omega_3,t_2,\omega_1)=\int_{-\infty}^{\infty}dt_3\int_{-\infty}^{\infty}dt_1 R_{ijkl}(t_3,t_2,t_1)\times\exp(-i(\omega_3 t_3+\omega_1 t_1)), \tag{13}$$

where $S_{ijkl}(\omega_3,t_2,\omega_1)$ is the complex signal and the indices $ijkl$ represent lab frame polarizations of the four fields.

Figure 3 shows the three pulse photon echo spectrum calculated using the parameters given in column four of Table I and Eq. (13). The homogeneous linewidth is equal to the experimentally measured[25] value of 2.6 cm^{-1} for all transitions and the polarizations of all four fields were taken to be parallel. Orientational factors were incorporated using Eq. (13) of Ref. 23. The spectral features can be interpreted in terms of transitions between the six lowest energy eigenstates. The fundamental and overtone transitions are clearly seen in the splitting of the diagonal peaks. The fundamental transitions at $(-\Omega_a,\Omega_a)$ and $(-\Omega_s,\Omega_s)$ correspond to the double-sided Feynman diagrams R_2 and R_3 depicted in Fig. 2, whereas the overtones are represented by the R_1^* path and appear in the off-diagonal at $(-\Omega_a,\Omega_a-\Delta_{aa})$ and $(-\Omega_s,\Omega_s-\Delta_{ss})$. Consistent with the harmonic approximation, the overtone peaks are approximately $\sqrt{2}$ times as intense as the fundamentals. The cross peaks, i.e., peaks resulting from intermode coupling, can be interpreted similarly. Peaks seen at $(-\Omega_a,\Omega_s)$ and $(-\Omega_s,\Omega_a)$ are represented by the diagrams R_2 and R_3 Fig. 2, whereas contributions from the R_1^* path show up as anharmonically shifted peaks at $(-\Omega_a,\Omega_s-\Delta_{as})$ and $(-\Omega_s,\Omega_a-\Delta_{as})$. However, the peak at $(-\Omega_a,\Omega_s-\Delta_{as})$ is unresolved due to overlap with the stronger diagonal peak at $(-\Omega_a,\Omega_a)$.

V. DISCUSSION

The overall agreement between the calculated and experimental parameters is satisfactory. However, the energy splitting between the singly excited eigenstates must be improved. Preliminary calculations of small peptides are much better in this regard, suggesting that the results of the present

work may be limited by the presence of the rhodium atom, which requires the introduction of a partially semiempirical basis set. Indeed, an accurate description of the electronic structure in the vicinity of the rhodium atom is expected to be critical in describing the mechanical coupling between the two C≡O local oscillators. The molecule has an interesting delocalized charge distribution (see Fig. 1) and other vibrations that are strongly coupled to the charges may affect the spectra.

Even though the computed bilinear coupling coefficient differs by a factor of ~ 2 from experiment we believe that our conclusions drawn regarding the effects of quartic terms hold, because anharmonicities and harmonically allowed transition dipole amplitudes are relatively insensitive to this parameter. For example, substitution of the V_{12} coefficient from Ref. 25 into our quartic DFT potential (Table I) results in the energies $\Omega_a = 1901.7\ \mathrm{cm}^{-1}$, $\Omega_s = 1972.1\ \mathrm{cm}^{-1}$, $\Delta_{aa} = 10.2\ \mathrm{cm}^{-1}$, $\Delta_{ss} = 8.4\ \mathrm{cm}^{-1}$, and $\Delta_{as} = 20.7\ \mathrm{cm}^{-1}$, where all anharmonicities change by less than $5.5\ \mathrm{cm}^{-1}$ from the values obtained with the DFT bilinear coupling coefficient. Furthermore, the transition dipole magnitudes for all harmonically allowed transitions change by less than 1% upon substitution. However, the transition dipole amplitudes between states that differ by more than one quanta (harmonically forbidden) change by less than 11% with the exception of $\mu_{a,ss}$ and $\mu_{s,aa}$, which both decrease by about 58%. Thus, the underestimation of the bilinear coupling coefficient by DFT is primarily manifested in the energy splitting of the eigenstates and the harmonically forbidden singly to doubly excited state transition dipoles.

In order to better evaluate our calculated parameters with respect to empirical values, we performed a fit to the experimental transition energies and dipoles of Ref. 25 using quartic expansion coefficients as adjustable parameters. Initially, a model in which the only nonzero anharmonic terms were diagonal cubic and quartic coefficients (g_{iii} and g_{iiii}) was used to achieve convergence to within $2\ \mathrm{cm}^{-1}$ of the experimental energies. However, we found that small g_{iij} and g_{iijj} parameters must be introduced to converge within $1\ \mathrm{cm}^{-1}$. Our final fitting parameters are $\omega_1 = \omega_2 = 2083\ \mathrm{cm}^{-1}$, $V_{12} = 34\ \mathrm{cm}^{-1}$, $g_{iii} = g_{jjj} = -229\ \mathrm{cm}^{-1}$, $g_{iij} = g_{ijj} = -1.5\ \mathrm{cm}^{-1}$, $g_{iiii} = g_{jjjj} = 31\ \mathrm{cm}^{-1}$, $g_{iiij} = g_{ijjj} = 0\ \mathrm{cm}^{-1}$, and $g_{iijj} = -0.3\ \mathrm{cm}^{-1}$, resulting in transition dipoles that differ by less than 2.5% from those shown in column four of Table I.

The dominant effect of including quartic terms is the increase in the transition dipoles between eigenstates that differ by two quanta. This point is illustrated by Fig. 4, a linear absorption spectrum calculated in the overtone region. The inclusion of quartic terms increases the ground to doubly excited states absorbance cross sections by 10%–30%. Similar effects could be observed in nonlinear experiments where the absorbance between excited states that differ by two quanta is probed; transient grating or two-color photon echo experiments are possibilities.[9] Our transition dipoles between the singly and triply excited levels are 20%–30% greater than those calculated using the parameters of Ref. 25.

To describe the spectroscopy of larger molecules the explicit treatment of more coordinates is required. The computational cost, however, increases rapidly for the determination of anharmonic force constants as well as for the (complete) diagonalization of the vibrational Hamiltonian. The latter step can be improved by implementing Krylov space based routines such as the Lanczos algorithm that do not diagonalize the full Hamiltonian, but calculate individual eigenstates sequentially.[73] Other procedures such as time-dependent Hartree method can be used to generate approximate eigenstates.[74] Alternatively, a perturbative approach that takes the effect of higher excitations into account could be utilized. The size of the basis can also be reduced by defining linear combinations of internal coordinates, although this requires at least partial abandonment of the more intuitive internal coordinates.

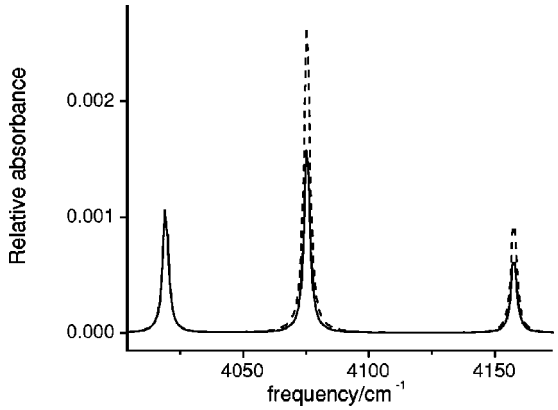

FIG. 4. Linear absorption spectra of RDC in the overtone region calculated using both our empirical fitting parameters (— — —) and those of Ref. 25 (—). Our final fitting parameters are $\omega_1 = \omega_2 = 2083\ \mathrm{cm}^{-1}$, $V_{12} = 34\ \mathrm{cm}^{-1}$, $g_{iii} = g_{jjj} = -229\ \mathrm{cm}^{-1}$, $g_{iij} = g_{ijj} = -1.5\ \mathrm{cm}^{-1}$, $g_{iiii} = g_{jjjj} = 31\ \mathrm{cm}^{-1}$, $g_{iiij} = g_{ijjj} = 0\ \mathrm{cm}^{-1}$, and $g_{iijj} = -0.3\ \mathrm{cm}^{-1}$. The intensities are normalized to the peak absorption of the symmetric fundamental.

ACKNOWLEDGMENTS

The support of NIH Grant No. GM59230-01A2 and NSF Grant No. CHE-0132571 is gratefully acknowledged. J.D. would like to thank the Max-Kade foundation for financial support of his stay in Rochester.

APPENDIX: TRANSFORMING PARAMETERS OF THE HAMILTONIAN

In normally ordered form, the creation operators are moved to the left of the annihilation operators in all operator products. Expressing the coordinates as normal ordered field operators results in the most convenient form for program implementation. Most generally, products of field operators can be normal ordered using

$$(\mu B_m + \nu B_m^\dagger)^n = \sum_{k=0}^{n} \binom{n}{k} \mu^k \left(\frac{ic}{2}\right) \mu^{n-k} H_{n-k} \times \left(\frac{\nu}{ic} B_m^\dagger\right) (B_m)^k, \tag{A1}$$

where H_{N-k} is a Hermite polynomial and $c = (2\mu\nu)^{1/2}$.[75] Substituting Eqs. (4) and (5) into Eq. (1) and normal ordering the terms results in Eq. (7), where the expansion coefficients are given by

$$U_m = U_m^{(1)} + 3\sum_n^{3N-6} U_{mnn}^{(3)}, \tag{A2}$$

$$h_{mn} = \delta_{mn}\left(\omega_m + 6\sum_p^{3N-6} U_{mnpp}^{(4)}\right) + (1-\delta_{mn})\left(U_{mn}^{(2)} + 6\sum_p^{3N-6} U_{mnpp}^{(4)}\right), \tag{A3}$$

$$U_{mn} = U_{mn}^{(2)} + 6\sum_p^{3N-6} U_{mnpp}^{(4)}, \tag{A4}$$

$$U_{mnp} = U_{mnp}^{(3)}, \tag{A5}$$

$$U_{mnpq} = U_{mnpq}^{(4)}, \tag{A6}$$

$$U_{k1k2\cdots kn}^{(n)} = \frac{f_{k1k2\cdots kn}^{(n)}}{\sqrt{2m_{k1}\omega_{k1}\hbar^{-1}2m_{k2}\omega_{k2}\hbar^{-1}\cdots 2m_{kn}\omega_{kn}\hbar^{-1}}}. \tag{A7}$$

Intrinsic frequencies ω_i of the internal coordinates are calculated using the diagonal elements of the second-order harmonic force constant matrix by

$$\omega_k = \frac{1}{2\pi c}\sqrt{\frac{f_{kk}}{m_k}}. \tag{A8}$$

Effective masses for internal coordinates m_k are taken directly from reciprocal diagonal elements of the Wilson G matrix ($m_k = G_{kk}^{-1}$)[76] provided by the quantum chemical programs. More sophisticated determinations of intrinsic frequencies have been put forward in the literature.[77–81]

Using Eq. (4) and neglecting the constant term, which has no effect on the spectra, Eq. (3) can be recast as Eq. (8), where

$$D_m^{(1)} = \sqrt{\frac{\hbar}{2m_m\omega_m}}\left(\frac{\partial\vec{\mu}}{\partial R_m}\right)_{R_m=0}. \tag{A9}$$

The x, y, and z components of the transition dipole were calculated.

[1] R. R. Ernst, G. Bodenhausen, and A. Wokaun, *Principles of Nuclear Magnetic Resonance in One and Two Dimensions* (Clarendon, Oxford, 1987).
[2] *Protein NMR Spectroscopy: Principles and Practice*, edited by J. Cavanagh, W. J. Fairbrother, I. Palmer, and G. Arthur (Academic, San Diego, 1996).
[3] S. F. Lienen, T. Bremi, B. Brutscher, R. Brüschweiler, and R. R. Ernst, J. Am. Chem. Soc. **120**, 9870 (1998).
[4] S. Mukamel and R. Hochstrasser, eds., Special issue on Multidimensional Spectroscopies, Chem. Phys. **266**, 135 (2001).
[5] H. Hamaguchi and T. Kitagawa, eds., Proceedings of TRVS 2001, special issue in Bull. Chem. Soc. Jpn **75**, 883 (2002).
[6] S. Mukamel, Annu. Rev. Phys. Chem. **51**, 691 (2000).
[7] Y. Tanimura and S. Mukamel, J. Chem. Phys. **99**, 9496 (1993).
[8] J. D. Hybl, J. Christophe, and D. M. Jonas, Chem. Phys. **266**, 295 (2001).
[9] O. Golonzka, M. Khalil, N. Demirdöven, and A. Tokmakoff, Phys. Rev. Lett. **86**, 2154 (2001).
[10] M. Khalil and A. Tokmakoff, Chem. Phys. **266**, 213 (2001).
[11] C. Scheurer and S. Mukamel, J. Chem. Phys. **115**, 4989 (2001).
[12] P. Hamm, M. Lim, W. F. DeGrado, and R. M. Hochstrasser, Proc. Natl. Acad. Sci. U.S.A. **96**, 2036 (1999).
[13] M. T. Zanni, N.-H. Ge, Y. S. Kim, and R. M. Hochstrasser, Proc. Natl. Acad. Sci. U.S.A. **98**, 11265 (2001).
[14] O. Golonzka, N. Demirdöven, M. Khalil, and A. Tokmakoff, J. Chem. Phys. **113**, 9893 (2000).
[15] A. Tokmakoff, J. Phys. Chem. A **104**, 4247 (2000).
[16] W. Zhao and J. C. Wright, Phys. Rev. Lett. **84**, 1411 (2000).
[17] M. Khalil, N. Demirdöven, O. Golonzka, C. J. Fecko, and A. Tokmakoff, J. Phys. Chem. A **104**, 5711 (2000).
[18] K. M. Murdoch, N. J. Condon, W. Zhao, D. M. Beseman, K. A. Meyer, and J. C. Wright, Chem. Phys. Lett. **335**, 349 (2001).
[19] N.-H. Ge, M. T. Zanni, and R. M. Hochstrasser, J. Phys. Chem. A **106**, 962 (2001).
[20] K. Okumura and Y. Tanimura, Chem. Phys. Lett. **278**, 175 (1997).
[21] K. Okumura, A. Tokmakoff, and Y. Tanimura, Chem. Phys. Lett. **314**, 488 (1999).
[22] K. Okumura, A. Tokmakoff, and Y. Tanimura, J. Chem. Phys. **111**, 492 (1999).
[23] R. M. Hochstrasser, Chem. Phys. **266**, 273 (2001); M. T. Zanni, S. Gnanakaren, J. Stenger, and R. M. Hochstrasser, J. Phys. Chem. B **105**, 6520 (2001).
[24] O. Golonzka and A. Tokmakoff, J. Chem. Phys. **115**, 297 (2001).
[25] O. Golonzka, M. Khalil, N. Demirdöven, and A. Tokmakoff, J. Chem. Phys. **115**, 10814 (2001).
[26] V. Capek and E. Silinsh, *Organic Molecular Crystals: Interaction, Localization, and Transport Phenomena* (AIP Press, New York, 1994).
[27] H. Torii and M. Tasumi, J. Chem. Phys. **96**, 3379 (1992).
[28] S. Tretiak, W. M. Zhang, V. Chernyak, and S. Mukamel, Proc. Nat Acad. Sci. **96**, 13003 (1999); S. Tretiak, C. Middleton, V. Chernyak, and S. Mukamel J. Phys. Chem. B **104**, 4519 (2000).
[29] S. Mukamel, *Principles of Nonlinear Optical Spectroscopy* (Oxford University Press, New York, Oxford, 1995).
[30] C. Lee and R. G. Yang, and W. Parr, Phys. Rev. B **37**, 785 (1988).
[31] B. Miehlich, A. Savin, H. Stoll, and H. Preuss, Chem. Phys. Lett. **157**, 200 (1989).
[32] A. D. Becke, J. Chem. Phys. **98**, 5648 (1993).
[33] R. H. Hertwig and W. Koch, Chem. Phys. Lett. **268**, 345 (1997).
[34] P. J. Hay and W. R. Wadt, J. Chem. Phys. **82**, 270 (1985).
[35] W. R. Wadt and P. J. Hay, J. Chem. Phys. **82**, 284 (1985).
[36] P. J. Hay and W. R. Wadt, J. Chem. Phys. **82**, 299 (1985).
[37] A. G. Császár, in *The Encyclopedia of Computational Chemistry*, edited by P. Schleyer, N. Allinger, T. Clark, J. Gasteiger, P. A. Kollman, H. A. Schaefer III, and P. R. Schreiner (Wiley, Chichester, 1998), pp. 13–30.
[38] J. Pipek and P. G. Mezey, Chem. Phys. **90**, 4916 (1989).
[39] J. Singh, *Excitation Energy Transfer Processes in Condensed Media: Theory and Applications* (Plenum, New York, 1994).
[40] R. Venkatramani and S. Mukamel, J. Chem. Phys. (to be published).
[41] S. Hahn, K. Park, and M. Cho, J. Chem. Phys. **111**, 4121 (1999).
[42] K. Park, M. Cho, S. Hahn, and D. Kim, J. Chem. Phys. **111**, 4131 (1999).
[43] M. Cho, J. Chem. Phys. **111**, 4140 (1999).
[44] H. Matsuura and H. Yoshida, in *Handbook of Vibrational Spectroscopy* (Wiley, Chichester, 2002), Vol. 3, pp. 2012–2028.
[45] H. Hotokka, in Ref. 44, Vol. 3. pp. 2029–2039.
[46] P. Pulay, G. Fogorasi, P. Pongor, J. E. Boggs, and A. Vargha, J. Am. Chem. Soc. **105**, 7037 (1983).
[47] G. Fogorasi and P. Pulay, Annu. Rev. Phys. Chem. **35**, 191 (1984).
[48] R. G. Parr and W. Yang, *Density-Functional Theory of Atoms and Molecules* (Oxford University Press, New York, 1989).
[49] B. G. Johnson, P. M. W. Gill, and J. A. Pople, J. Chem. Phys. **98**, 5612 (1993).
[50] G. Rauhut and P. Pulay, J. Phys. Chem. **99**, 3093 (1995).
[51] A. Scott and L. Radom, J. Phys. Chem. **100**, 16502 (1996).
[52] M. W. Wong, Chem. Phys. Lett. **256**, 391 (1995).
[53] T. Sundius, Vib. Spectrosc. **29**, 89 (2000).
[54] M. A. Palafox and V. K. Rastogi, Spectrochim. Acta, Part A **58**, 411 (2002).
[55] H. Yoshida, A. Ehara, and H. Matsuura, Chem. Phys. Lett. **325**, 477 (2000).
[56] H. Yoshida, K. Takeda, J. Okamura, A. Ehara, and H. Matsuura, J. Phys. Chem. **106**, 3580 (2002).
[57] B. S. Galabov and T. Dudev, *Vibrational Intensities* (Elsevier Science, Amsterdam, 1996), Vol. 22.
[58] Y. Yamaguchi, M. Frisch, J. Gaw, H. F. Schaefer III, and J. Binkley, J. Chem. Phys. **84**, 2262 (1986).
[59] B. Galabov, P. Bobadova-Parvanova, and T. Dudev, J. Mol. Struct. **406**, 119 (1997).

[60] B. Galabov, Y. Yamaguchi, R. B. Remington, and H. F. Schaefer III, J. Phys. Chem. A **106**, 819 (2002).
[61] M. W. Schmidt, K. K. Baldridge, J. A. Boatz *et al.*, J. Comput. Chem. **14**, 1347 (1993).
[62] M. J. Frisch, G. W. Trucks, H. B. Schlegel, G. E. Scuseria, M. A. Robb, J. R. Cheeseman, V. G. Zakrzewski, J. A. Montgomery, R. E. Stratmann, J. C. Burant, *et al.*, GAUSSIAN 98 *Revision A.9*, Gaussian, Inc., Pittsburgh PA 1998.
[63] J. Gauss, in *Modern Methods and Algorithms in Quantum Chemistry*, edited by J. Grotendorst (John von Neumann Institute for Computing, Jülich, 2000), Vol. 3, pp. 541–592.
[64] B. J. Crawford, J. Chem. Phys. **20**, 977 (1952).
[65] T. A. Ford and D. Steele, Spectrochim. Acta, Part A **55**, 2823 (1999).
[66] E. R. Bernstein, S. D. Colson, R. Kopelman, and G. W. Robinson, J. Chem. Phys. **48**, 5596 (1968).
[67] P. N. Prasad and R. Kopelman, J. Chem. Phys. **57**, 856 (1972).
[68] R. Kopelman, in *Excited States*, edited by E. C. Lim (Academic, New York, 1975), Vol. 2.
[69] D. M. Alexander and J. A. Krumhansl, Phys. Rev. B **33**, 7172 (1986).
[70] A. C. Scott, Phys. Rep. **217**, 1 (1992).
[71] J. Edler and P. Hamm, J. Chem. Phys. **117**, 2415 (2002).
[72] A. Gbureck, W. Kiefer, M. E. Schneider, and H. Werner, Vib. Spectrosc. **17**, 105 (1998).
[73] B. Parlett, *Symmetric Eigenvalue Problem* (Prentice–Hall, Englewood Cliffs, 1980).
[74] R. Gerber and M. Ratner, Adv. Chem. Phys. **70**, 70 (1988).
[75] A. Wünsche, J. Opt. B: Quantum Semiclassical Opt. **1**, 264 (1999).
[76] E. B. Wilson Jr., J. C. Decius, and P. C. Cross, *Molecular Vibrations* (Dover, New York, 1955).
[77] J. A. Boatz and M. S. Gordon, J. Phys. Chem. **93**, 1819 (1989).
[78] Z. Konkoli and D. Cremer, Int. J. Quantum Chem. **67**, 1 (1998).
[79] Z. Konkoli, A. Larsson, and D. Cremer, Int. J. Quantum Chem. **67**, 11 (1998).
[80] Z. Konkoli and D. Cremer, Int. J. Quantum Chem. **67**, 29 (1998).
[81] Z. Konkoli, A. Larsson, and D. Cremer, Int. J. Quantum Chem. **67**, 41 (1998).